

Nonlinear effects in the propagation of surface magnetostatic waves in yttrium iron garnet films in weak magnetic fields

P. E. Zil'berman, V. M. Kulikov, V. V. Tikhonov, and I. V. Shein

Institute of Radio Engineering and Electronics, Academy of Sciences of the USSR

(Submitted 10 September 1990)

Zh. Eksp. Teor. Fiz. **99**, 1566–1578 (May 1991)

The propagation of surface magnetostatic waves in (111) yttrium iron garnet films was studied experimentally in weak tangential magnetic fields \mathbf{H}_0 at frequencies from 200 MHz to 3 GHz. The attenuation of a wave transmitted through the film was measured as a function of the input power P of the wave and the orientation of \mathbf{H}_0 with respect to the crystallographic axes. Wave propagation in a direction perpendicular to \mathbf{H}_0 was observed in two field intervals. The first was an interval of weak fields, "transparency window I" [P. E. Zil'berman *et al.*, Radiotekh. Elektron. **32**, 710 (1987)]. This interval is typically $3 \lesssim H_0 \lesssim 15$ Oe. In this interval, the attenuation is independent of P for any orientation of \mathbf{H}_0 . The second interval is at fields $H_0 > 25$ –40 Oe, where the attenuation does depend on P . The dependence varies with the frequency. It changes markedly with a change in the orientation of \mathbf{H}_0 . If \mathbf{H}_0 is oriented along a [110] direction and is close to the limiting value, $H_0 = 25$ –20 Oe, there is a certain field interval in which there is a pronounced broadening of the frequency range in which the wave attenuation is nearly independent of P . This is "transparency window II." Outside window II the attenuation increases very rapidly with increasing P . For other orientations of \mathbf{H}_0 , there is no window II. These observations are interpreted as evidence of single-step and two-step decays of a surface wave which are strongly influenced by the magnetic anisotropy of the film. This interpretation is supported by the observation of an anisotropic nucleation of new waves at the exit, with frequencies differing from that of the incident wave.

1. INTRODUCTION AND STATEMENT OF THE PROBLEM

The magnetostatic waves (MS waves) propagating in layers of ferromagnets are customarily subdivided into surface magnetostatic waves (SMS), backward bulk magnetostatic waves (BBMS), and forward bulk magnetostatic waves (FBMS). The distinction between backward and forward waves is essentially based on the sign of the projection of the group velocity $v_{gr} = \partial\omega(\mathbf{q})/\partial\mathbf{q}$ onto the direction of the phase velocity $\mathbf{v}_{ph} = \omega\mathbf{q}/q^2$; i.e., it is based on the sign of the product $\omega\mathbf{q}\partial\omega/\partial\mathbf{q}$, where \mathbf{q} and $\omega(\mathbf{q})$ are the wave vector and angular frequency of the MS wave. For BBMS waves we thus have $\omega\mathbf{q}\partial\omega/\partial\mathbf{q} < 0$, while for FBMS waves we have $\omega\mathbf{q}\partial\omega/\partial\mathbf{q} > 0$ (Ref. 1).

Surface and backward bulk magnetostatic waves were first observed in plane-parallel plates (or films) of isotropic ferromagnets in a saturating magnetic field \mathbf{H}_0 by Damon and Eshbach.² Forward bulk magnetostatic waves were first observed by Bar'yakhtar and Kaganov.³ It turns out that whether a given type of MS wave can propagate depends on the orientation of the vector \mathbf{H}_0 with respect to the plate and on the orientation of the vector \mathbf{q} with respect to \mathbf{H}_0 (by definition, the vector \mathbf{q} always lies in the plane of the plate). When the field \mathbf{H}_0 is oriented in the plane of the plate (such fields are "tangential"), parallel to \mathbf{H}_0 ($\mathbf{q} \parallel \mathbf{H}_0$), only BBMS waves can propagate; if it is instead oriented perpendicular to \mathbf{H}_0 ($\mathbf{q} \perp \mathbf{H}_0$), only SMS waves can propagate. In a tangential field \mathbf{H}_0 , FBMS waves cannot exist at all, regardless of the direction of \mathbf{q} . If the field \mathbf{H}_0 is instead oriented along the normal to the plane of the plate (this is the case of a "normal" field \mathbf{H}_0), only FBMS waves can propagate, regardless of the direction of \mathbf{q} . The propagation of these waves is isotropic, i.e., independent of the direction of \mathbf{q} .

When the magnetic anisotropy of the ferromagnet is taken into account, the picture becomes considerably more complex, as has been shown in several studies.⁴⁻⁷ In particular, waves of all types (SMS, BBMS, and FBMS) can in principle propagate simultaneously in a tangential field \mathbf{H}_0 with $\mathbf{q} \perp \mathbf{H}_0$. This possibility is illustrated by Fig. 1 and will be discussed in more detail below.

The SMS waves have attracted particularly great interest, for many reasons. In particular, these waves belong to the only isolated branch in the spectrum of natural magnetic excitations of a plate. These waves are predicted theoretically to be strictly surface waves if one ignores the energy of the nonuniform exchange interaction of the magnetic moments at neighboring points in the medium.^{8,9} That simplification is justified in studies of waves with values of q which are not too large (under the condition $Dq^2 \ll 1$, where D is the nonuniform-exchange constant) and in plates (or films) of sufficiently large thickness d (e.g., $d > 4 \mu\text{m}$), with a weak pinning of the spins at the surfaces.¹⁰ In this exchange-free approximation, the energy flux in a wave results solely from the magnetic dipole interaction. As a result it turns out that this flux is essentially zero except in a limited interval of the wave number q , specifically,

$$0 \leq q \leq 1/2d. \quad (1)$$

The frequency interval $f \equiv \omega/2\pi$, in which magnetic-dipole SMS waves can propagate, turns out to be limited in a corresponding way. For waves in a plate of an isotropic material this interval is

$$[f_H(f_H + f_m)]^{1/2} \leq f \leq (f_H + 1/2f_m), \quad (2)$$

where $f_H = \gamma H_0$ and $f_m = 4\pi\gamma M_0$, M_0 is the saturation

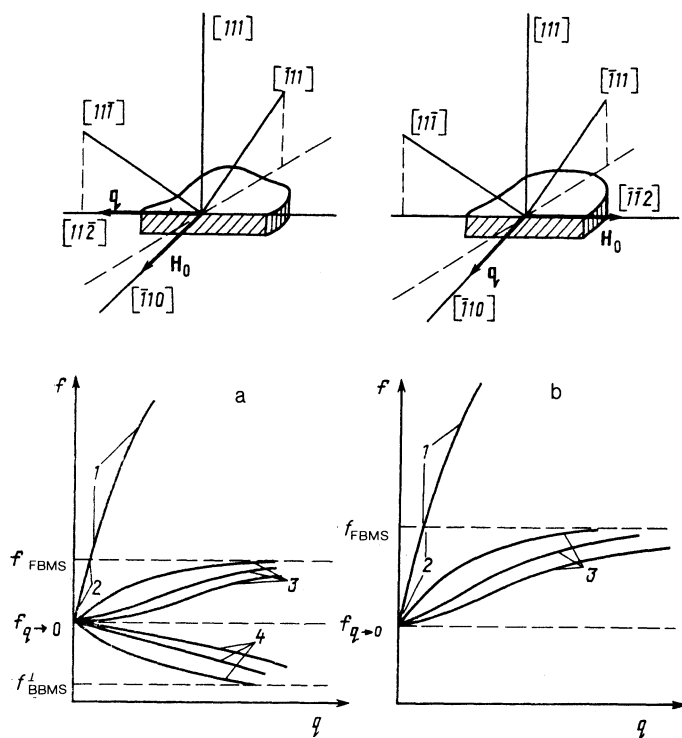


FIG. 1. Orientation of the field H_0 and of the wave vector q with respect to the crystallographic axes of the film, along with dispersion curves for (1) surface magnetostatic waves, (2, 3) forward bulk magnetostatic waves, and (4) backward bulk magnetostatic waves. a) For angles $\varphi = 0^\circ + n \cdot 60^\circ$; b) $\varphi = 30^\circ + n \cdot 60^\circ$.

magnetization of the ferromagnet, and γ is the gyromagnetic ratio. Substituting the parameter values¹¹ typical of yttrium iron garnet (YIG) films into (2), we find the following estimates of the boundaries of interval (2) for the region of weak magnetic fields in which we are interested here, $H_0 = 3-100$ Oe:

$$\begin{aligned} [f_H(f_H + f_m)]^{1/2} &\sim 200-1220 \text{ MHz}, \\ (f_H + 1/2 f_m) &\sim 2500-2770 \text{ MHz}. \end{aligned} \quad (3)$$

Incorporating the magnetic anisotropy results in only a slight shift (Sec. 3) of the boundaries of interval (2); this interval continues to exist, the propagation zones are the same, and estimates (3) of the limiting frequencies remain in force. Limitations of similar meaning on the values of q and f can be found for the other types of MS waves (BBMS and FBMS).

At a sufficiently lower power P of an SMS wave, at which the propagation is linear, dissipative processes govern the attenuation of a wave passing through a film. With increasing P , however, nonlinear attenuation mechanisms may also come into play; an example is the decay of an SMS wave into waves of other types. In some cases the nonlinear attenuation is so pronounced that it leads to a complete suppression of the wave at certain frequencies. As a result, the frequency limits seen experimentally on the interval of existence of SMS waves are not approximately the same as those which are found from (2); they are instead limits set by the conditions under which decay processes are forbidden.¹¹

The nonlinear attenuation of SMS waves was first studied by Schilz.¹² The SMS waves were excited and detected by two transducers consisting of systems of parallel metal strips on the YIG film; a microwave current could propagate along these strips. The field H_0 was directed parallel to the strips, and the vector q perpendicular to H_0 . The ratio of the output

power P' to the input power P was studied as a function of P . It was found that this ratio decreases with increasing P when P is above a certain threshold P_0 . Mednikov¹³ observed yet another effect at $P > P_0$: the appearance at the output of signals with frequencies tens of megahertz away from the frequency f of the microwave input signal. All these effects were studied in detail experimentally by Temiryazev¹⁴ and were explained as resulting from an instability of an SMS wave with respect to decays into two BBMS waves.

Melkov and Sholom¹⁵ have recently studied other manifestations of the same instability of an SMS wave: a "cleavage" of the microwave pulse exciting the SMS wave and an emission of electromagnetic waves, which are decay products at frequencies close to $f/2$. Reaching an understanding of the processes by which SMS waves decay in YIG films is important for reasons going beyond the effort to explain the manifestations of the instability. Gusev *et al.*¹⁶ showed experimentally that at low power levels, $P < P_0$, i.e., below the instability threshold, these processes contribute substantially to the damping rate of SMS waves, and they explain its nonmonotonic frequency dependence. The decays of SMS waves have not been studied adequately on the theoretical side, apparently because of difficulties in describing nonlinear waves in plates. The only general approach to the solution of this problem which has been developed is that by Preobrazhenskiĭ *et al.*,¹⁷ to the best of our knowledge.

So far, all the research on nonlinear effects during the propagation of SMS waves has used YIG films in a strong saturating field H_0 ($H_0 \gtrsim 300$ Oe). The study which we are reporting here is a further development of experiments on decays of SMS waves in YIG films. For the first time, a study has been made of the propagation of intense SMS waves in weak fields H_0 (in some cases, nonsaturating fields)—on the order of and weaker than the magnetic-anisotropy fields in the film. At such fields, conditions favor decays of SMS

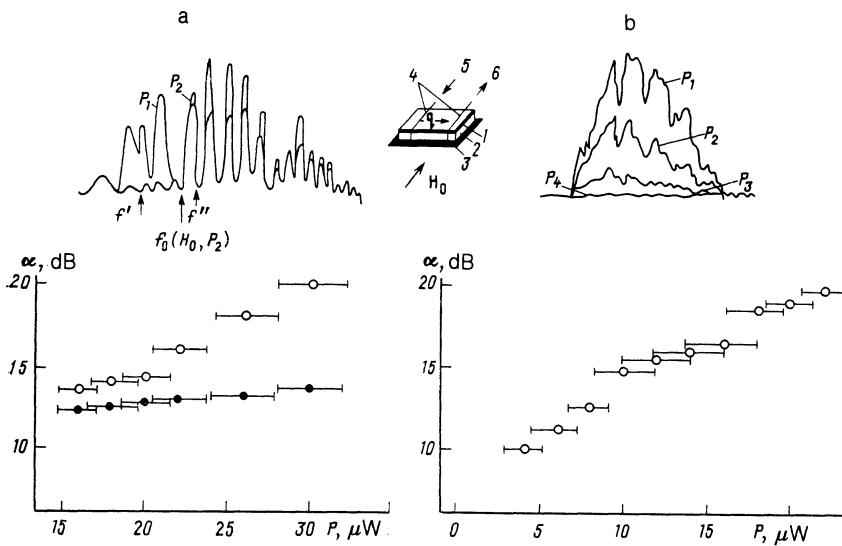


FIG. 2. Amplitude-frequency characteristics and plot of the attenuation α of the magnetostatic waves which have traversed a YIG film versus the input power P for angles $\varphi = 0^\circ + n \cdot 60^\circ$. a: Field $H_0 = 50$ Oe. Open points— $\alpha(P)$ for a frequency $f' = 1500$ MHz; filled points— $f'' = 1700$ MHz. Shown at the top is the amplitude-frequency characteristic of the sample for MS-wave input power levels $P_1 = 16 \mu\text{W}$ and $P_2 = 30 \mu\text{W}$ in the frequency range 1180–2200 MHz. b: $H_0 = 300$ Oe. Open points—For a frequency $f = 2420$ MHz. Shown at the top is the amplitude-frequency characteristic of the sample with $P_1 = 4 \mu\text{W}$, $P_2 = 8 \mu\text{W}$, $P_3 = 16 \mu\text{W}$, and $P_4 = 30 \mu\text{W}$ over the range 2230–2864 MHz. Inset: Experimental layout. 1—YIG film; 2—GGG substrate; 3—metal base; 4—metal strips of transducers; 5,6—input and output for rf power.

waves, since these decays are allowed by energy conservation over the entire frequency range in which these waves exist. The anisotropy has a strong effect on the spectrum of magnetic waves at these fields. As we will see below, this circumstance leads to some interesting new features in the course of the decay processes. To a large extent, these features determine the very possibility that SMS waves will propagate in weak fields H_0 .

2. TEST SAMPLES AND MEASUREMENT PROCEDURE

The test samples were epitaxial YIG films grown on gadolinium-gallium garnet (GGG) substrates in a (111) plane. The films ranged in thickness d from 4 to 40 μm ; the width of the resonance line was $2\Delta H \leq 0.5$ Oe. The orientations of the crystallographic axes of the films were determined by x-ray diffraction. A domain structure was observed in polarized light in the films at fields $H_0 \leq 40$ Oe. This domain structure consisted of an irregular distribution of blocks of stripe domains, as described in detail in Ref. 18. The MS waves were excited and detected with transducers consisting of metal strips 20 μm wide and 1 mm long, separated by a distance of 1.5 mm. Each strip was grounded at one end. The other ends of the strips were connected either to the microwave source (in the case of the input transducer)

or to a microwave detector (for the output transducer). Strip transducers of this sort are capable of efficiently exciting and detecting only those MS waves which are propagating along the perpendicular to the strips.¹⁹ In these experiments the external magnetic field H_0 was directed along the strips in all cases, so we can assume that the vectors \mathbf{q} and \mathbf{H}_0 were mutually perpendicular: $\mathbf{q} \perp \mathbf{H}_0$ (see the inset in Fig. 2).

Panoramic instruments were used as the microwave sources and detectors over the frequency range from 200 MHz to 3 GHz. Specifically, we used standing-wave-ratio and attenuation meters for which the power level which could be generated was 3 mW or 1.5 μW and could be adjusted by inserting attenuators. The power level P of the MS signal was found as the difference between the power levels of the microwave signal incident on the sample and of that reflected from the sample. The lower frequency f_0 of the observed MS waves, was measured. The accuracy of these measurements was limited by interference oscillations resulting from the superposition of electromagnetic stray pickup and the MS-wave signals at the output transducer. The inset in Fig. 3 illustrates the procedure which we used to measure the lower frequency f_0 and to estimate the error Δf of these measurements. The lower frequencies measured for the MS waves by this method are shown by the points in

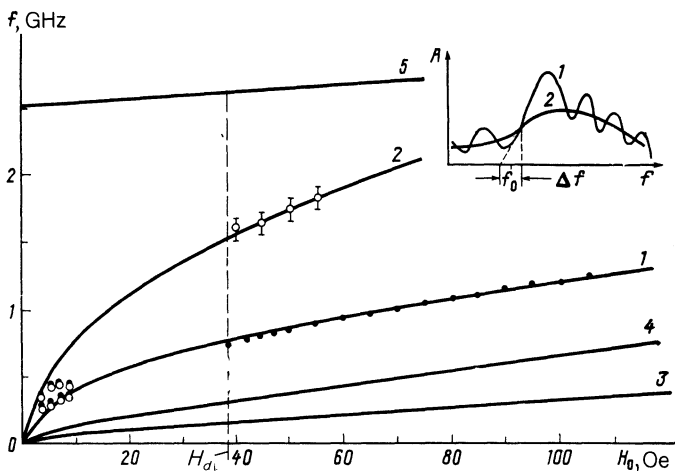


FIG. 3. Limiting wave frequencies versus the field H_0 at $\varphi = 30^\circ$. The lines show calculated boundary frequencies. 1— $f_{q-0}(H_0)$; 2— $2f_{q-0}(H_0)$; 3— $f_{\text{BBMS}}^{\parallel}(H_0)$; 4— $2f_{\text{BBMS}}^{\parallel}(H_0)$; 5— $f_{\text{SMS}}(H_0)$. The points are the measured limiting frequencies of surface magnetostatic waves (at fields $H_0 < 15$ Oe, all the frequencies at the boundary of the region in which the waves are observed; at fields $H_0 > 39$ Oe, only the lower boundary frequencies). Filled circles— $P = 1 \mu\text{W}$; open circles— $P = 1 \text{mW}$. The inset illustrates the method used to measure the lower limiting frequency of the surface magnetostatic waves. 1) Amplitude-frequency characteristic of the sample (A is the amplitude, and f the frequency); 2) amplitude-frequency characteristic averaged over the oscillations. Here f_0 is the lower limiting frequency of the surface magnetostatic waves, and Δf is an estimate of the error in the determination of this lower limiting frequency.

Figs. 3 and 4. At low power levels ($P \sim 1 \mu\text{W}$), the size of the error corresponds to the size of the filled points ($\Delta f/f_0 \sim 5\%$), while at high power levels ($P \sim 1 \text{mW}$) the error is greater, represented by the vertical error bars on the open points ($\Delta f/f_0 \sim (10-15)\%$).

3. EXPERIMENTAL RESULTS

As the magnetic field H_0 is raised from zero, propagation of MS waves in the test samples can be observed over the interval $3 \lesssim H_0 \lesssim 15 \text{ Oe}$ at frequencies f on the order of 250–400 MHz. These waves are similar to the waves described in Ref. 18, where this interval of magnetic fields was called a “transparency window.” This window, which we will call “transparency window I,” exists for any orientation of the film with respect to the transducers. As the power P is raised, the attenuation of the MS waves in window I does not change. This result suggests that the propagation of the waves is linear within window I for all values of P attainable in our experiments.

With a further increase in H_0 , the propagation of MS waves can be observed again, starting at fields of 25–40 Oe and continuing to higher fields. The domain structure which is observed disappears at $H_0 \approx H_d = 36-39 \text{ Oe}$. In these fields, the MS waves can propagate regardless of whether there is a domain structure.

The P dependence of the attenuation of MS waves in these fields is considerably more complex than in window I. In the first place, the dependence varies with the frequency. Second, it is anisotropic, by which we mean that it varies with the orientation of the film with respect to H_0 . We denote by φ the angle between H_0 and the [110] axis, which lies in the plane of the film (Fig. 1). For all angles $\varphi \neq 0^\circ + n \cdot 60^\circ$, where $n = 0, 1, \dots, 5$, an increase in P results in a substantial attenuation of the MS waves at frequencies in the lower part of the propagation band, no more than an octave above the lower frequency limit $f_0^{\text{min}}(H_0)$ on the MS-wave spectrum measured at a low power $P \lesssim 1 \mu\text{W}$. At these frequencies, at $P \approx 20 \mu\text{W}$ in films with $d \lesssim 20 \mu\text{m}$, the MS wave is essentially indistinguishable against the noise level. In thicker films, the wave is 15–20 dB weaker than at $P \sim 1 \mu\text{W}$. The results suggest that the lower limit itself becomes a function of not only the field H_0 but also the power P : $f_0 = f_0(H_0, P)$. This lower limit increases with increasing P

at a fixed H_0 . At sufficiently high power levels ($P \geq 100 \mu\text{W}$) are sufficient for films with any thickness d in the interval 4–40 μm , it reaches a limiting value $2f_0^{\text{min}}(H_0)$. At frequencies $f > 2f_0^{\text{min}}(H_0)$, the attenuation is essentially independent of P at all the power levels used ($< 3 \text{mW}$).

When we consider angles $\varphi = 0^\circ + n \cdot 60^\circ$, we see that there exists a field interval $[H_{01}, H_{02}]$ in which the lower frequency $f_0(H_0, P)$ either is totally independent of P or increases, at the P values attainable, to a certain maximum $f_0^{\text{max}}(H_0) < 2f_0^{\text{min}}(H_0)$. In other words, it increases by less than an octave. At frequencies $f > f_0^{\text{max}}(H_0)$ the attenuation of the MS waves is independent of (or nearly independent of) P . We call this field interval “transparency window II.” For any field H_0 inside window II, i.e., for $H_{01} < H_0 < H_{02}$, there exists a frequency band

$$f_0^{\text{max}}(H_0) < f < 2f_0^{\text{min}}(H_0) \quad (4)$$

within which the propagation of the MS waves is linear, since the attenuation does not depend on P . If we consider a frequency f satisfying condition (4) at some value of H_0 in window II, and if we measure the attenuation at this frequency at fields $H_0 > H_{02}$, i.e., outside window II, we find that this attenuation increases strongly with increasing P . In other words, there is a nonlinear suppression of the wave. The lower boundary H_{01} of window II, is approximately $H_d - 10 \text{ Oe}$, and the upper boundary, H_{02} , is on the order of 40–55 Oe and independent of H_d . We find no dependence of H_{01} or H_{02} on the film thickness. As we move away from $\varphi = 0^\circ + n \cdot 60^\circ$, the field H_{02} decreases sharply, while the field H_{01} increases; this increase is always slower than the decrease in H_{02} . At $\varphi = \pm 10^\circ + n \cdot 60^\circ$, window II essentially disappears.

To find more details on this effect and to find an explanation for it, we studied a film with $d \approx 6.3 \mu\text{m}$. The experimental results and estimates below refer to that film. A domain structure was observed in that film at $H_0 < H_d \approx 38 \text{ Oe}$; window I was $3 \lesssim H_0 \lesssim 13 \text{ Oe}$; and window II at $\varphi = 0^\circ$ was $25 \lesssim H_0 \lesssim 55 \text{ Oe}$. Shown at the top in Fig. 2a, and b, is the typical amplitude-frequency characteristic, i.e., the typical plot of the attenuation of the SMS signal at the output transducer as a function of the frequency. The amplitude-frequency characteristic in Fig. 2a was obtained at an H_0 value inside window II, and that in Fig. 2b was obtained at a much

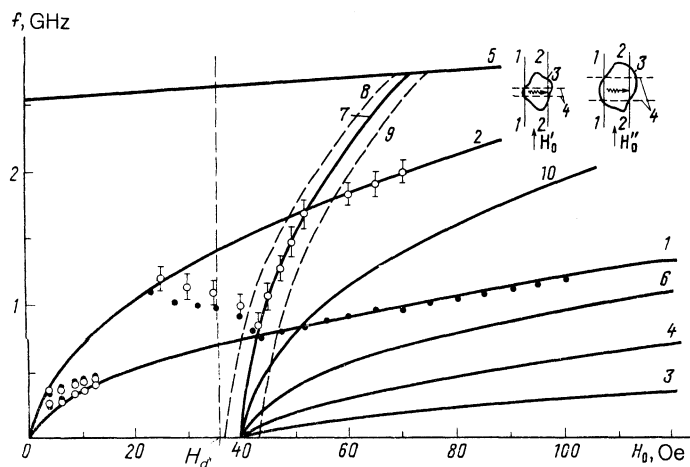


FIG. 4. Limiting wave frequencies versus the field H_0 for $\varphi = 0^\circ$. The lines are calculated limiting frequencies: 1— $f_{q=0}(H_0)$; 2— $2f_{q=0}(H_0)$; 3— $f_{\text{BBMS}}^{\parallel}(H_0)$; 4— $2f_{\text{BBMS}}^{\parallel}(H_0)$; 5— $f_{\text{BBMS}}(H_0)$; 6— $f_{\text{BBMS}}^{\perp}(H_0)$; 7— $4f_{\text{BBMS}}^{\perp}(H_0)$; 8,9—limits on the error in the theoretical calculation of dispersion curve 7; 10— $2f_{\text{BBMS}}^{\perp}(H_0)$. The points are the measured limiting frequencies of the surface magnetostatic waves. Filled points— $P = 1 \mu\text{W}$; open points— $P = 1 \text{mW}$. The inset illustrates the possibility for a surface magnetostatic wave to go from input transducer (1) to output transducer (2) within a single block of stripe domains (3). Dashed lines 4 show a track along which surface magnetostatic waves propagate without being scattered by the block boundaries ($H_0' < H_0''$).

higher value of H_0 , far outside this window. We see that at fields H_0 within window II we can specify a certain limiting or boundary frequency $f_0(H_0, P_2) \approx f_0^{\max}(H_0)$, since P_2 is fairly high, $30 \mu\text{W}$. At MS-wave frequencies $f > f_0(H_0, P_2)$, the attenuation either does not increase at all or increases only slightly with increasing P . At MS-wave frequencies $f < f_0(H_0, P_2)$, the attenuation increases rapidly with increasing P .

These results are illustrated in Fig. 2a by two curves of the attenuation versus P , constructed from the corresponding amplitude-frequency characteristics for two specific frequencies, f' and f'' . Similar amplitude-frequency characteristics were found outside but not too far from window II, specifically, at $H_{02} < H_0 \leq 100$ Oe. There is the distinction that outside window II the limiting or boundary frequencies $f_0^{\max}(H_0)$ are higher, equal to $2f_0^{\min}(H_0)$ in all cases. The limiting or boundary frequencies for all other orientations of the film ($\varphi \neq 0^\circ + n \cdot 60^\circ$), at which window II did not exist at any field value H_0 , behaved in precisely the same way. It can be seen from Fig. 2b that far outside window II, at $H_0 \approx 300$ Oe, the limiting or boundary frequencies are not observed at all: They have risen above the upper limiting frequency of the MS-wave spectrum. In this case we observe only a monotonic increase in the attenuation with increasing P at all frequencies in the propagation band. At fields $H_0 > 25\text{--}40$ Oe, for arbitrary angles φ , the upper frequency boundary for the observation of MS waves is on the order of 2.2–2.4 GHz, in rough correspondence with the calculated upper boundary frequency for SMS waves.

4. DISCUSSION

An attempt might be made to explain the observations described in the preceding section of this paper—a P -dependent attenuation of MS waves, which is nonuniform over frequency and anisotropic, and transparency window II—in terms of decay processes accompanying the propagation of intense SMS and FBMS waves in a YIG film. One must bear in mind here that the magnetic anisotropy of the film strongly influences these processes in weak fields H_0 .

Before we could find this explanation, we needed to determine the anisotropy parameters and the magnetization M_0 of the test samples. For this purpose, we used the method described in Ref. 20. We found the uniaxial-anisotropy constant $2\beta/M_0$ and the quantity $4\pi M_0$ from two sets of experimental data: (1) measurements of that frequency $f_{q \rightarrow 0}$ in the wave spectrum which corresponds to the wave number $q \rightarrow 0$ as a function of the field H_0 when this field is oriented along the normal to the film surface and (2) measurements of the wave dispersion curves for a tangential orientation of the field H_0 with respect to the surface of the film, at various values of φ . As a result we found $4\pi M_0 = 1760 \pm 10$ G and $2\beta/M_0 = 0 \pm 10$ G. Since the measured wave dispersion curves did not change when we rotated the film 120° with respect to the transducers, we concluded that the anisotropy axis in the sample is not substantially tilted with respect to the normal.

The cubic-anisotropy field K_1/M_0 was found from the measured dependence of the frequency $f_{q \rightarrow 0}$ on the angle φ in a film magnetized at an acute angle with respect to the surface (i.e., in a "skew-magnetized film").²¹ It was found to be $K_1/M_0 \approx -40$ Oe. This value of K_1/M_0 corresponds to the

results of other measurements.^{22–24} According to data in the literature,^{22,23} the second cubic-anisotropy constant satisfies $|K_2| \ll |K_1|$ ($K_2/M_0 \approx -2$ Oe). We accordingly assumed that the K_2 contribution had no substantial effect on the positions of the limiting frequencies in the wave spectrum. The error of these estimates does not exceed the errors in the measurements of the limiting frequencies, which amount to 5–15% (see curves 7–9 in Fig. 4).

We need next some computational information on the wave spectrum in the film, with allowance for the anisotropy, with the parameter values which we determined. For simplicity we limit the discussion to the spectrum of the magnetic-dipole (exchange-free) waves, which are of primary importance for films with thicknesses $d > 4 \mu\text{m}$, as we mentioned back in Sec. 1. We can make use of the dispersion relation from Ref. 21 for magnetic-dipole waves. It is expedient to begin with a discussion of simple analytic expressions for the limiting frequencies of the spectrum; these expressions are found from the equation which we just mentioned under the single condition $\mathbf{M}_0 \parallel \mathbf{H}_0$. Although this condition does not hold rigorously in weak fields, a subsequent rigorous numerical calculation (a far more laborious undertaking) justifies the use of these analytic expressions for drawing general conclusions about the properties of the spectrum.

We assume $\mathbf{q} \perp \mathbf{H}_0$. In addition to the SMS waves, which are present even if we ignore the anisotropy, we also find BBMS and FBMS waves as a result of the anisotropy. The dispersion curves for all types of waves are monotonic, and nearly all lie between the two limiting frequencies reached as $q \rightarrow 0$ and $q \rightarrow \infty$. All three of these wave types (SMS, BBMS, and FBMS) have the same limiting frequency $f_{q \rightarrow 0}$ as $q \rightarrow 0$:

$$f_{q \rightarrow 0} = [R - f_c^2 (\cos 6\varphi + 1)]^{1/2}, \quad (5)$$

where $R = f_H(f_H + f_m + f_a)$, $f_a = f_{0a} - f_c$, $f_{0a} = \gamma 2\beta/M_0$, and $f_c = \gamma K_1/M_0$. The limiting frequencies in the case $q \rightarrow \infty$ are

$$f_{\text{SMS}} = f_H + 1/2(f_m + f_a), \quad (6)$$

$$f_{\text{BBMS}}^{\perp} = \{R - f_c^2 (\cos 6\varphi + 1) + 1/2 f_H [f_a - [f_a^2 + 4f_c^2 (\cos 6\varphi + 1)]^{1/2}]\}^{1/2}, \quad (7)$$

$$f_{\text{FBMS}} = \{R - f_c^2 (\cos 6\varphi + 1) + 1/2 f_H [f_a + [f_a^2 + 4f_c^2 (\cos 6\varphi + 1)]^{1/2}]\}^{1/2}. \quad (8)$$

For the BBMS waves, which exist at $\mathbf{q} \parallel \mathbf{H}_0$, the limiting frequency as $q \rightarrow 0$ is given by (5), and the limiting frequency as $q \rightarrow \infty$ is

$$f_{\text{BBMS}}^{\parallel} = [(f_H + f_a)f_H - f_c^2 (\cos 6\varphi + 1)]^{1/2}. \quad (9)$$

It can be seen from (7) and (8) that for $\varphi = 30^\circ + n \cdot 60^\circ$ one of the frequencies f_{BBMS}^{\perp} , f_{FBMS} is the same as $f_{q \rightarrow 0}$. At $f_a < 0$, the frequencies f_{FBMS} and $f_{q \rightarrow 0}$ are the same, while at $f_a > 0$ the frequencies f_{BBMS}^{\perp} and $f_{q \rightarrow 0}$ are the same. The condition $f_a > 0$ held in our samples (since $\beta > 0$ and $K_1 < 0$), so the frequency band in which BBMS waves exist vanishes at this value of φ . In contrast, at $\varphi = 0^\circ + n \cdot 60^\circ$, this band becomes the widest. The FBMS waves exist at arbitrary φ .

Figure 1 shows the shape of the dispersion curves for waves with $\mathbf{q} \perp \mathbf{H}_0$ according to these calculations. One of the curves (specifically, curve 2) for the FBMS waves crosses limiting frequency f_{FBMS} at a finite q and converts smoothly into dispersion curve 1 for the SMS waves. Consequently, a single dispersion curve describes one of the FBMS modes (curve 2) at small values of q , and at large values of q one dispersion curve describes one of the SMS modes (curve 1). At all values of q , this dispersion curve, 1, 2, lies in the frequency band $\Delta_{1,2}f \equiv f_{\text{SMS}} - f_{q=0}$. The other dispersion curves for the FBMS waves (curve 3) lie in the frequency band $\Delta_3f \equiv f_{\text{FBMS}} - f_{q=0}$ for all q , while curves 4 for the BBMS waves lie in the band $\Delta_4f \equiv f_{q=0} - f_{\text{BBMS}}$. Under our experimental conditions, the relations $(f_H/f_m)^{1/2} \lesssim 0,3 \ll 1$, $f_a/f_m \lesssim 10^{-1} \ll 1$, and $|f_c|/f_m \lesssim 10^{-1} \ll 1$ held. Using these relations and (5)–(8), we find

$$\frac{\Delta_3f}{\Delta_{1,2}f} \lesssim \frac{1}{2} \left(\frac{f_H}{f_m} \right)^{1/2} \frac{(f_a^2 + 8f_c^2)^{1/2} + f_a}{f_m} \sim 10^{-2} \ll 1, \quad (10)$$

$$\frac{\Delta_4f}{\Delta_{1,2}f} \lesssim \frac{1}{2} \left(\frac{f_H}{f_m} \right)^{1/2} \frac{(f_a^2 + 8f_c^2)^{1/2} - f_a}{f_m} \sim 10^{-2} \ll 1. \quad (11)$$

Since the frequency bands Δ_3f and Δ_4f turn out to be relatively narrow, the group velocities of the corresponding waves are relatively small, so it is legitimate to ignore the propagation of these waves from the input transducer to the output transducer. The group velocities found for curves 3 and 4 turn out to be lower by a factor of 10–100 than those for curves 1 and 2. Correspondingly, the wave propagation times and damping rates are related in the same way. It has thus been established that the signal detected by the output transducer is determined primarily by SMS waves and by those FBMS waves which belong to dispersion curve 2. For brevity we will speak in terms of the SMS waves, with the understanding that these may also be FBMS waves at small values of q .

Let us compare the limiting frequencies $f_0(H_0, P)$ found experimentally for the SMS spectrum at various power levels P with the calculated limiting frequencies. For this purpose we will use not the approximate expressions (5)–(9) but the results of a rigorous numerical solution of the dispersion relations from Ref. 21, without any simplifying assumptions regarding the relative orientation of \mathbf{M}_0 and \mathbf{H}_0 . The lines in Figs. 3 and 4 show the limiting frequencies calculated for various angles φ . At sufficiently small values of H_0 , the experimental points define a region in the (H_0, f) plane in which the propagation of SMS waves is observed. We see that this region exists for arbitrary angles φ . It corresponds to transparency window I. We note two points: First, the boundaries of this region are essentially independent of P (the open and filled points are superimposed on each other). Second, window I lies at $H_0 < H_d$, i.e., in a region in which a domain structure exists.

Zil'berman *et al.*¹⁸ linked the appearance of window I with a linear propagation of SMS waves in a film with an irregular domain structure. Such a film can be regarded as homogeneous on the average, since the wavelength of the SMS waves is considerably larger than the greatest size of the irregularities, i.e., the typical size of a block of domains. Figures 3 and 4 contain some additional information in support of this interpretation. We see that with increasing H_0 , it is

primarily waves with the largest wave numbers q [those farthest from the lower limiting frequency $f_{q=0}(H_0)$] which go outside the region (H_0, f) in the plane corresponding to window I, in which the propagation of SMS waves is observed. This is as it should be, since (first) the sizes of the blocks increase with H_0 , and (second) it is primarily for the largest values of q that the wavelength is comparable to the increasing dimensions of the blocks.

The lower limiting frequencies of the SMS waves at fields $H_0 \gtrsim 25\text{--}40$ Oe, in contrast with those in window I, are characterized by a pronounced anisotropy, as can be seen from a comparison of these frequencies in Figs. 3 and 4. In Fig. 3 ($\varphi = 30^\circ$), at the lowest power levels P (the filled points), the lower frequencies of SMS waves, $f_0^{\text{min}}(H_0)$, lie on calculated curve $f_{q=0}(H_0)$. As P increases, however, the signal is attenuated strongly in the lower-frequency part of the spectrum, as is shown in detail in Fig. 2a. As a result, at $P = 1$ mW the lower limiting frequencies increase (the open points), and—an extremely important point—they become superimposed on the curve of $2f_{q=0}(H_0)$. In other words, the limiting frequency $f_0(H_0, P_2)$ shown in Fig. 2a is approximately equal to $2f_{q=0}(H_0)$. In this orientation, this is the behavior of the lower limit in all the films studied.

We believe that the increase in the attenuation of the SMS waves with increasing P at the frequencies $f_{q=0} < f < 2f_{q=0}$ is due to a decay of an intense SMS wave into two BBMS waves which propagate in a direction nearly parallel to \mathbf{H}_0 . This decay is completely the same in nature as that described in Refs. 13 and 14. In accordance with Ref. 25, we found the threshold for this decay to be $\lesssim 1 \mu\text{W}$. At frequencies $f > 2f_{q=0}$ this decay is forbidden by the conservation laws: The frequencies of the waves which are the decay products lie outside the spectrum of BBMS waves.²⁾ It is natural to suggest that this is the reason why the lower limiting frequency $f_0(H_0, P)$ of the spectrum of SMS waves shifts to $2f_{q=0}(H_0)$, as we observed in the experiments as P was increased. This effect is specific to the decays of SMS waves in weak fields H_0 . It could not be observed in Refs. 12–16, for example, because the fields there were $H_0 \gtrsim 300$ Oe. At such strong fields H_0 , the frequency $2f_{q=0}(H_0)$ went outside the spectrum of SMS waves (it lay above the upper limiting frequency of this spectrum).

We now consider the lower limiting frequencies in Fig. 4 ($\varphi = 0^\circ$). At $H_0 \gtrsim 55$ Oe, these frequencies could in principle be at precisely the same positions as in Fig. 3. Specifically, at low values $P \sim 1 \mu\text{W}$ (the filled points) they would be superimposed on the $f_{q=0}(H_0)$ curve, while at high values $P \sim 1$ mW (the open points) they would be superimposed on the $2f_{q=0}(H_0)$ curve. Correspondingly, the explanation of this position is the same as that above. In the interval $25 \lesssim H_0 \lesssim 55$ Oe, however, which we mentioned back in Sec. 2, where we called it “transparency window II,” there are substantial differences. Specifically, there is a V-shaped dip in the lower boundary, which is particularly sharp at large values of P . At $P \sim 1$ mW the right-hand boundary of this dip is superimposed on the $4f_{\text{BBMS}}^\perp(H_0)$ curve. This fact suggests the following explanation for the right-hand boundary: At $2f_{q=0}(H_0) > f > 4f_{\text{BBMS}}^\perp(H_0)$, there can be a two-step process. In the first step, there is a decay (which we have already discussed) of an SMS wave into two BBMS waves, which propagate in the direction parallel to \mathbf{H}_0 . In the sec-

ond step, the BBMS waves excited in the decay of the SMS wave themselves decay, forming two new BBMS waves, which propagate in a direction nearly perpendicular to \mathbf{H}_0 . The latter BBMS waves do indeed exist at $\varphi = 0^\circ$, as can be seen from Fig. 1a. In addition, it is at $\varphi = 0^\circ$ that the frequency band for the existence of these waves is at its broadest. This interpretation also explains the absence of a similar dip at $\varphi = 30^\circ$. At such values of φ the frequency band in which the BBMS waves exist is zero, as can be seen from Fig. 1b. Since the second step of the process reduces the amplitude of the BBMS waves propagating in the direction parallel to \mathbf{H}_0 , the threshold for the instability of the SMS waves should rise (the stimulated decays of SMS waves should slow down). We would expect that this circumstance would end or slow the increase in the attenuation of the SMS waves with increasing P . This is precisely the behavior which we observe in window II (Fig. 1a).

We would like to know the explanation for the left-hand boundary of the V -shaped dip in Fig. 4. We first note that the position of this boundary depends weakly on P . We believe that this boundary is determined by an effect of the domain structure. One might suggest two mechanisms for such an effect. First, the fine-scale stripe domain structure inside the domain blocks¹⁸ could lead to an effective scattering of the BBMS waves which are propagating along a direction perpendicular to \mathbf{H}_0 and also perpendicular to the domain walls. This scattering would raise the threshold in the second step of the decay process and would thus accelerate the decays of SMS waves in the first step. The effect would be to shift the boundary upward, closer to the $2f_{q=0}(H_0)$ curve, above which the decays are forbidden. Evidence for this mechanism comes from the fact that the left-hand boundary depends (albeit weakly) on P . Second, it is entirely possible¹⁸ that the dimensions of certain of the domain blocks at $H_0 \sim 25\text{--}50$ Oe would be comparable to the distance between

the input and output transducers (~ 1.5 mm). The SMS waves might then travel from the input transducer to the output transducer without leaving a given block. As H_0 increases, the size of the opposing regions of the transducers which are spanned by the block should increase (see the inset in Fig. 4). Correspondingly, SMS waves with progressively greater wavelengths would become capable of propagating from the input to the output without being scattered by block boundaries. This effect could explain the behavior of the left-hand boundary as a function of H_0 , i.e., the shift of this boundary toward the $f_{q=0}(H_0)$ curve with increasing H_0 .

These ideas regarding the nonlinear anisotropic decay processes find further support in our observation of yet another effect. This effect was observed in films of the greater thickness, $d \approx 40 \mu\text{m}$, at $P \approx 4 \mu\text{W}$, in the region bounded by the $2f_{q=0}(H_0)$ and $2f_{\text{BBMS}}^{\pm}(H_0)$ curves in the (H_0, f) plane in (Fig. 5a). This effect consists of the appearance at the output transducer of—in addition to the signal at the original frequency—signals at frequencies slightly separated from the original frequency (satellites). At $4 \lesssim P \lesssim 10 \mu\text{W}$ these frequencies form a discrete spectrum, while at $P > 10 \mu\text{W}$ they form a continuum. Figure 5, b and c, shows some typical spectrograms for two values of the power P . In principle, this effect appears to be analogous to the creation of satellite frequencies as described in Refs. 13 and 14. However, the region in which the effect occurs, shown by the hatching in Fig. 5a, provide evidence that in this case there is apparently a decay of an SMS wave into two BBMS waves, which propagate along a direction perpendicular to \mathbf{H}_0 , rather than along \mathbf{H}_0 , as in Refs. 13 and 14. Since BBMS waves with $\mathbf{q} \perp \mathbf{H}_0$ exist only as a result of the anisotropy, the effect which we observed is very anisotropic. It is observed at those orientations of \mathbf{H}_0 (at values of φ near 0°) at which transparency window II is observed.

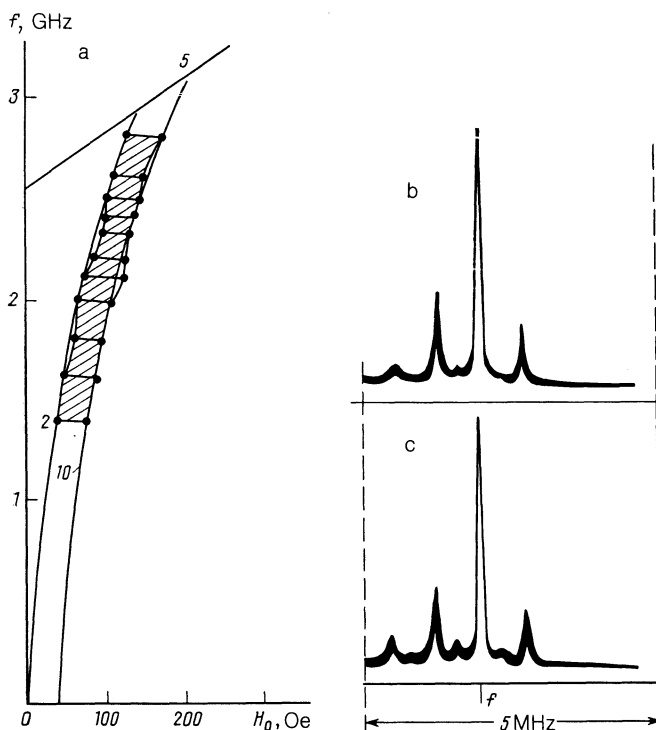


FIG. 5. a—The region (hatched) within which signals at frequencies different from the frequency of the signal applied to the input are observed at the output transducer, at a sufficiently high input power P (the numbers labeling the curves correspond to those in Fig. 4); b,c—typical patterns on the screen of the spectrum analyzer, for $H_0 = 76$ Oe and $f = 2160$ MHz (b— $P = 4 \mu\text{W}$; c— $P = 5 \mu\text{W}$).

In summary, in weak magnetizing fields the very possibility that SMS waves will propagate in YIG films is determined by two factors: the domain structure and the nonlinear decay processes, which are strongly influenced by the magnetic anisotropy. The results of this study show the need for the derivation of a theory for the propagation of surface magnetostatic waves of finite intensity in anisotropic ferrite films of the YIG type in the presence and absence of an irregular domain structure in the films.

We are deeply indebted to Yu. V. Gulyaev for interest in this work and to A. G. Temiryazev for interesting discussions.

¹⁾In YIG ($Y_3Fe_5O_{12}$), these parameter values are $D = 2.6 \cdot 10^{-12} \text{ cm}^2$, $\gamma = 2.83 \text{ MHz/Oe}$, and $4\pi M_0 = 1760 \text{ G}$.

²⁾As was mentioned in Ref. 16, the boundaries of the regions in which the decay processes occur are determined only by degenerate decays.

¹J. D. Adam and J. H. Collins, Proc. IEEE **64**, 794 (1976).

²R. W. Damon and J. R. Eshbach, J. Phys. Chem. Solids **19**, 308 (1961).

³V. G. Bar'yakhtar and M. I. Kaganov, *Nonuniform Resonances and Spin Waves* [in Russian], Fizmatgiz, Moscow, 1961, p. 266.

⁴A. S. Beregov, Izv. Vyssh. Uchebn. Zaved., Radiofiz. **26**, 363 (1983).

⁵S. A. Byzulin, *Abstract, Candidate's Dissertation*, Moscow State University, Moscow, 1983.

⁶O. L. Galkin and P. E. Zil'berman, Pis'ma Zh. Tekh. Fiz. **10**, 1077 (1984) [Sov. Tech. Phys. Lett. **10**, 456 (1984)].

⁷R. G. Kryshchal' and A. V. Medved', Zh. Tekh. Fiz. **57**, 1936 (1987) [Sov. Phys. Tech. Phys. **32**, 1165 (1987)].

⁸L. N. Bulaevskii, Fiz. Tverd. Tela (Leningrad) **12**, 799 (1970) [Sov. Phys. Solid State **12**, 619 (1970)].

⁹R. E. De Wames and T. Wolfram, J. Appl. Phys. **41**, 987 (1970).

¹⁰Yu. V. Gulyaev, P. E. Zil'berman, and A. V. Lugovskoi, Fiz. Tverd. Tela (Leningrad) **23**, 1136 (1981) [Sov. Phys. Solid State **23**, 660 (1981)].

¹¹A. M. Mednikov, A. L. Galanin, Yu. V. Gulyaev *et al.*, Fiz. Tverd. Tela (Leningrad) **23**, 2116 (1981) [Sov. Phys. Solid State **23**, 1234 (1981)].

¹²W. Schilz, Philips Res. Rep. **28**, 50 (1973).

¹³A. M. Mednikov, Fiz. Tverd. Tela (Leningrad) **23**, 242 (1981) [Sov. Phys. Solid State **23**, 136 (1981)].

¹⁴A. G. Temiryazev, Fiz. Tverd. Tela (Leningrad) **29**, 313 (1987) [Sov. Phys. Solid State **29**, 179 (1987)].

¹⁵G. A. Melkov and S. V. Sholom, Zh. Eksp. Teor. Fiz. **96**, 712 (1989) [Sov. Phys. JETP **69**, 403 (1989)].

¹⁶B. N. Gusev, A. G. Gurevich, A. N. Anisimov *et al.*, Fiz. Tverd. Tela (Leningrad) **28**, 2969 (1986) [Sov. Phys. Solid State **28**, 1669 (1986)].

¹⁷V. L. Preobrazhenskii, V. P. Rybakov, and Yu. K. Fetisov, Radiotekh. Elektron. **33**, 1218 (1988).

¹⁸P. E. Zil'berman, G. T. Kazakov, and V. V. Tikhonov, Radiotekh. Elektron. **32**, 710 (1987).

¹⁹A. B. Valyavskii, A. V. Vashovskii, K. V. Grechushkin, and A. V. Stal'makhov, Radiotekh. Elektron. **33**, 1830 (1988).

²⁰P. E. Zil'berman, V. M. Kulikov, V. V. Tikhonov, and I. V. Shein, Radiotekh. Elektron. **35**, 986 (1990).

²¹S. L. Vysotskii, G. T. Kazakov, Yu. A. Filimonov *et al.*, Radiotekh. Elektron. **35**, 959 (1990).

²²A. G. Gurevich, *Magnetic Resonances in Ferrites and Antiferromagnets* [in Russian], Nauka, Moscow, 1973.

²³O. A. Chivileva, A. G. Gurevich, and L. M. Émiryan, Fiz. Tverd. Tela (Leningrad) **29**, 110 (1987) [Sov. Phys. Solid State **29**, 61 (1987)].

²⁴A. V. Voronenko, S. V. Gerus, and L. A. Krasnozhen, Mikroelektronika **18**, 61 (1989).

²⁵O. A. Chivileva, A. G. Gurevich, A. N. Anisimov *et al.*, Fiz. Tverd. Tela (Leningrad) **29**, 1774 (1987) [Sov. Phys. Solid State **29**, 1020 (1987)].

Translated by D. Parsons